

On the Coupling of Vibrational Relaxation with the Dissociation–Recombination Kinetics: From Dynamics to Aerospace Applications[†]

M. Capitelli,^{‡,§} G. Colonna,[§] and F. Esposito^{*,§}

Dipartimento di Chimica, Università degli Studi, Bari, Italy, and Istituto di Metodologie Inorganiche e dei Plasmi, del C.N.R., Sezione di Bari, Italy

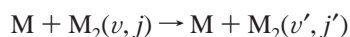
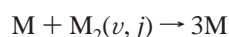
Received: March 15, 2004; In Final Form: June 4, 2004

A refined set of state-to-state dissociation cross sections for the process $N + N_2(v, j) \rightarrow 3N$ has been obtained by the quasiclassical trajectory (QCT) method and used in a 1D code describing the expansion of a dissociation–recombination mixture through a converging–diverging nozzle. The relevant vibrational kinetics includes V–V and V–T energy transfers as well as dissociation–recombination processes. The results show strong nonequilibrium vibrational distributions and non-Arrhenius dissociation rates along the nozzle axis as a consequence of the recombination process.

1. Introduction

Nonequilibrium vibrational kinetics is a topic of large interest due to its interconnection with plasmas, lasers, combustion systems, and aerospace technology. From the theoretical point of view, the topic received large improvement with the complete sets of vibration–vibration (V–V) and vibration–translation (V–T) rates calculated by Billing et al. many years ago^{1–2} and which are still taken as reference data for different applications. Since then, vibrational kinetics progressed also thanks to the efforts made by other groups to characterize cross sections involving atomic species.^{3–5} In particular, V–T cross sections involving atomic species are of paramount importance in such studies as well as the state-to-state dissociation cross sections of molecular species by atoms. Finally, gas phase and gas surface recombination rates complete the picture to model the vibrational kinetics under nonequilibrium conditions.⁶

In this paper, we present refined cross sections for the processes



where v and j represent in the order the vibrational and rotational quantum numbers.

Dissociation and vibration–translation (V–T) cross sections for the N_2 system, obtained by the quasiclassical trajectory method (QCT), have been refined by estimating the role of the triplet state of N_2 as well as by increasing the density of trajectories especially in the low-temperature range (less than 1000 K). Taking as inputs the new refined data, rate coefficients for the recombination have been calculated by detailed balance.

The refined state-to-state rates have been inserted in a 1D fluid dynamic code describing the expansion of a partially dissociated N_2 system through a convergent–divergent nozzle, this kind of study being important for aerospace applications.⁷ In this way, we are able to study the coupling of the vibrational

kinetics in the presence of dissociation–recombination processes under strong nonequilibrium conditions. Non-Boltzmann vibrational distributions and non-Arrhenius behavior of reaction rates along the nozzle coordinate appear as a result of selective pumping of vibrational quanta on the top of the vibrational ladder. The relevant results depend on the selection of input data, so that it appears interesting to compare the use of the QCT method with the well-known ladder climbing model, a dissociation model already used in ref 1.

2. Quasiclassical Calculations

To obtain a complete data set of detailed cross sections for dissociation and VT processes, the dynamical method adopted is QCT, a well-established technique that offers a good compromise between global reliability of results and computational time required, as tested in our preceding works^{4,5,8} on this topic. We actually performed a completely new set of calculations with respect to ref 4, using the same potential energy surface (PES),⁹ but applying a more accurate procedure of calculation. First of all, we have further developed our parallelized code for QCT, totally written in house,¹⁰ with very high parallel performance, due to the intrinsic independence of the calculation of different trajectories. This independence is successfully exploited by a very simple and efficient distribution of the computational load among processors: the master CPU assigns a batch of trajectories (typically 5–10 000) at each processor, which works writing the output directly to a file specified only for that processor. This very simple scheme has the great advantage of the portability over very different parallel and/or distributed computational environments, without requiring any kind of high performance node communication (the buffer normally present guarantees that the writing operation does not actually take place each time the processor writes virtually in the file). This kind of model is possible because each trajectory batch is written together with all the data needed to reconstruct the information for cross section calculation in a self-consistent “packet”. A series of several packets coming from any combination of processors/parallel-machine/cluster can be easily processed by the analysis program.¹⁰ The independence of the batches of trajectories is guaranteed by the independence of pseudorandom number generators used for different processors,

[†] Part of the “Gert D. Billing Memorial Issue”.

[‡] Università degli Studi.

[§] Istituto di Metodologie Inorganiche e dei Plasmi.

which is in turn obtained by using an algorithm in which not simply the starting point but also the pseudorandom sequence is controlled by four integer numbers. The parallelization is implemented using the well-known message passing interface (MPI) libraries.

We calculated by the WKB method the whole rovibrational ladder of $N_2(v, j)$ (about 10 000 states) supported by the PES, including quasibound states. Then we obtained cross sections for the whole rotational ladder connected to a given vibrational state, but only for one in five vibrational states, starting from $v = 0$, plus the last vibrational state $v = 67$ supported by the PES used. The rate coefficients from initial states not considered in QCT calculations are obtained by linear interpolation of the logarithm of the two rate coefficients with the nearest initial vibration. In contrast with our preceding procedure in ref 4, interpolation on vibration appears to be much easier and accurate than the one on rotation; actually we found it is needed if the interpolation is on cross sections and not on rate coefficients. In the former case, a rotationally averaged cross section can be extremely small at low temperature, but not zero even for low initial vibrational states, being a weighted sum over the whole rotational ladder, including very high states. This feature is of importance when considering the interpolation over the logarithm, because it practically circumvented the problem of dissociation thresholds. The importance of obtaining cross sections instead of rate coefficient is due to the use of these data in direct Monte Carlo codes where the kinetics of chemical systems is studied without the approximation of translational equilibrium (implicit in the definition of rate coefficient).

Another new aspect of these calculations with respect to ref 4 is the check for errors in the trajectory calculation. We now perform such check on every trajectory, by reintegration with a smaller time step, and up to 5–6 reiterations on check fail. The gain is not only in the accuracy of the calculations (only checked trajectories are saved, in contrast with the more common one-in-ten trajectory checking), but also in a significant reduction of computational time because we start with a relatively large initial time step, good for over 90% of the trajectories and obviously very cheap, spending only occasionally much more time (even 10–20 times larger) for very long and complex trajectories, obtaining a mean time for trajectory from 1.5 to 2 larger than that for trajectories good at the first attempt. This mean time is at most equal and often significant less than the one for calculations with a fixed time step calibrated for obtaining trajectories good at the first hit with a percentage very near to 100%.

We included in these calculations even quasibound (QB) states (classically bound by the rotational barrier, but over the dissociation limit), because they have large importance in dissociation/recombination kinetics.¹¹ In fact, these states have lifetimes very spread; therefore, a particular QB can be seen as stable if its lifetime is long in comparison with the mean time between consecutive atom–molecule collisions, and vice versa. Of course, this is a large kinetic problem that should be solved performing a study including QB and VT rates (vibration–translation) with specific conditions mimicking a particular experimental environment, as in ref 12 for hydrogen.

Another aspect of relevance of this new set of cross sections for nitrogen with respect to ref 4 is the consideration in an approximate way of dissociation from excited electronic states of N_2 , in particular, from states correlating with the same products (ground state of atomic nitrogen 4S) as for the PES used. Following and extending the approximation of Nikitin,¹³ as we did in ref 5, we consider an equilibrium between

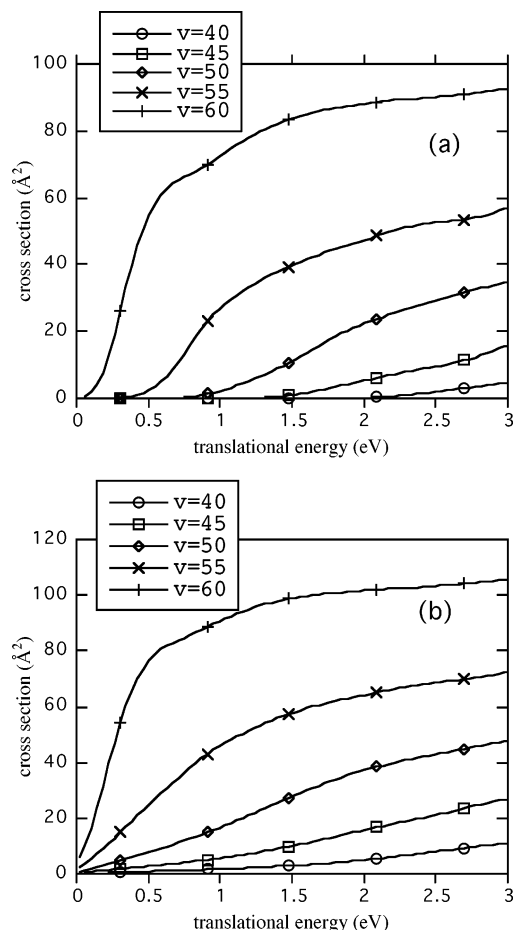


Figure 1. A sample of dissociation cross sections from the initial vibrational state indicated in the labels for (a) $T_r = 300$ K and (b) $T_r = 10\,000$ K. The correction factor for the triplet state is included (see text).

vibrational states of the ground electronic state and of those of comparable energy of any excited electronic state having a minimum less than the energies the vibrational states involved. Practically, we assign to a vibrational state v a multiplicity given by the sum, divided by the multiplicity of the ground electronic state, of the multiplicities of all the electronic states, correlating with the same products of the ground PES, having a minimum less than the energy of the state v . Considering nitrogen there is only a contribution from $A^3\Sigma_u^+$, that is, factor four starting from rovibrational states with energies larger than -3.59 eV (dissociation level is zero), considering that ground state is a singlet. This procedure has given good results if compared with global experimental data, as shown in ref 5.

In Figure 1a,b some samples of dissociation cross sections are shown, from initial vibrational states indicated in the legends. Cross sections are averaged with a rotational Boltzmann distribution at 300 and $10\,000$ K, respectively, in Figure 1a,b. The comparison shows not only an increasing of the maximum values of the cross sections, but also a large displacement of the thresholds toward lower values for the higher temperature. The translational energy range (from 10^{-3} to 3 eV) has been discretized in 75 bins. Cross sections are smoothed by fitting their logarithm with a local weighted least-squares procedure.⁵ This method consists of calculating in each point ϵ_0 on the energy axis a local fit with a polynomial of third degree on the 30 points nearest ϵ_0 , weighting the values with an exponential of the energy distance from ϵ_0 : $w(\epsilon) = -\exp(|\epsilon - \epsilon_0|/\Delta)$. This procedure is iterated twice, the first time with $\Delta = 0.05$ eV, and the second with $\Delta = 0.25$ eV.

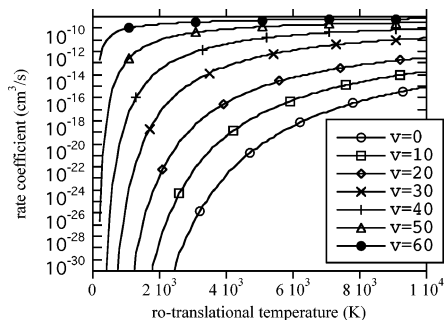


Figure 2. A sample of dissociation rate coefficients from the initial vibrational state in the legend as a function of ro-translational temperature.

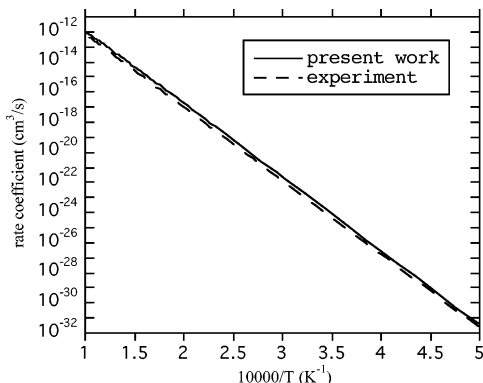


Figure 3. Comparison of thermal dissociation rates via QCT method (present work) and experimental data from ref 14.

Concerning dissociation rate coefficients, some examples are shown in Figure 2, starting from $v = 0$ up to $v = 60$, including the effect of the correction factor for the triplet state. These v -dependent rate coefficients have a rotational temperature equal to the translational one.

A validation of the present cross sections and rates can be performed by calculating the global thermal dissociation rate (see ref 8 for the procedure) for the process $N + N_2 \rightarrow 3N$ and comparing it as a function of temperature with the experimental results reported in ref 14. The agreement is globally good taking into account the difficulty in the experimental determination of dissociation rates, with our results larger (up to a maximum of 50%) in the examined temperature range (see Figure 3; note that our curve has been obtained with about 100 points uniformly distributed in whole range shown in the figure).

It is interesting to compare our rates for $N + N_2(v)$ with VT monoquantum de-excitation coefficients for $N_2(0) + N_2(v)$ from Billing² at 1000 and 4000 K, as a function of initial vibrational level v (see Figure 4). At 1000 K the two results show an increasing trend starting from similar values on $v = 1-2$, but rates for atom–molecule V–T become very rapidly higher than molecule–molecule V–T, with almost 1 order of magnitude at $v = 5$, almost 2 orders of magnitude for $v > 10$. At 4000 K, on the contrary, the discrepancy of 1 order of magnitude in favor of atom–molecule de-excitation rates is on the first vibrational levels, slowly decreasing up to negligible values for $v > 25$. The difference in the two sets of rates, which refer to different processes, are mainly due to the PES used in the two cases; in particular, the present calculation includes reactive (exchange) and inelastic channels, while only the inelastic process is included in the N_2-N_2 calculation.

3. Fluid Dynamic Model

In this section, we will briefly describe the general model for a reacting flow through a converging–diverging nozzle in

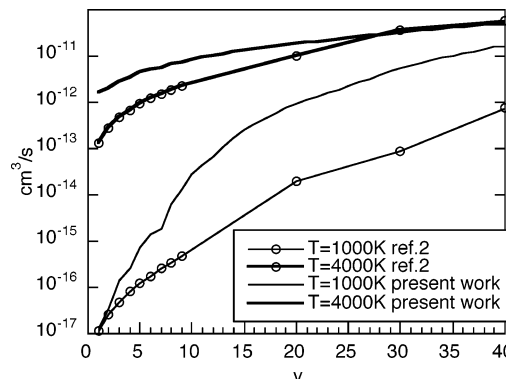


Figure 4. Comparison of monoquantum de-excitation VT rate coefficients for atom–molecule and molecule–molecule collisions at 1000 and 4000 K.

the quasi one-dimensional approximation and in stationary conditions.¹⁵ In this case, the Euler equations have the form:

$$\frac{d(\rho u A)}{dx} = 0 \quad \text{mass conservation}$$

$$\frac{dP}{dx} + \rho u \frac{du}{dx} = 0 \quad \text{momentum conservation}$$

$$u \frac{du}{dx} + \frac{dh_T}{dx} + \frac{dh_v}{dx} = 0 \quad \text{energy conservation}$$

$$\frac{d(\rho_{iv} u A)}{dx} = \dot{\rho}_{iv} \quad \text{chemical reactions}$$

$$P = \frac{\rho R T}{\bar{m}} \quad \text{state equation} \quad (1)$$

where x is the position coordinate along the nozzle axis, A is the nozzle section, ρ is the total mass density, and ρ_{iv} is the mass density of the i th species in the v th level, $\dot{\rho}_{iv}$ is the density production rate due to chemical processes, u is the flow speed, P is the hydrostatic pressure, T is the translational temperature, h_T and h_v are respectively the translational and the internal specific enthalpies, R is the ideal gas universal constant, and \bar{m} is the mean molar mass. The translational enthalpy h_T is proportional to the gas temperature according to the relation:

$$h_T = \frac{c_p}{\bar{m}} = \alpha \frac{R}{\bar{m}} T = \alpha R T \quad (2)$$

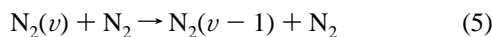
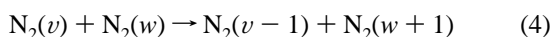
where c_p is the constant pressure molar specific heat and $\alpha = \gamma/(\gamma - 1)$ with $\gamma = c_p/c_v$, (c_v is the constant volume specific heat). The specific heat must be calculated considering only the contribution of the translational degrees of freedom and of the other degrees of freedom in equilibrium with it, while in the internal enthalpy h_v is taken into account all the others, included the chemical and the internal contribution (in our case, the molecular vibrational levels):

$$h_v = \frac{1}{\bar{m}} \sum_{iv} \chi_{iv} (H_i + \epsilon_{iv}) \quad (3)$$

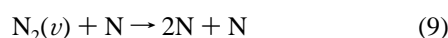
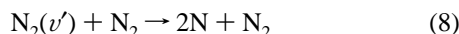
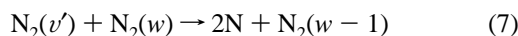
c_i and H_i are the molar fraction and the molar formation enthalpy of the i th species and χ_{ik} and ϵ_{ik} are the level distribution and energy.

The Euler equations can be rearranged as discussed in ref 15.

Let us now discuss the vibrational kinetics inserted in the nozzle equations for the N_2/N mixture. We have considered 68 vibrational levels of the nitrogen molecule submitted to the action of V–V and V–T energy exchanges processes (vibration–vibration V–V, vibration–translation by molecules V– T_m , vibration–translation by atomic nitrogen V– T_a),



The dissociation–recombination process is taken into account according to the ladder climbing model¹



where v' represents the last bound level of the molecule.

The rate coefficients for the processes (7, 8) are calculated in the ladder climbing approximation by extrapolating the bound-to-bound rates in the continuum.^{1,2} For the dissociation by atomic nitrogen (process 9), we have considered both the ladder climbing (LC) model and the QCT rates presented in this paper. The QCT rates have been fitted by the analytical function

$$\ln [k_{dv}(T)] = a_0 + a_1 e^{-T/b_1} - a_2 e^{-T/b_2} - a_3 e^{-T/b_3} - a_4 e^{-T/b_4} \quad (10)$$

where b 's are (in Kelvin degrees) $b_1 = 772.0459$; $b_2 = 243.6286$; $b_3 = 82.3776$; $b_4 = 3178.7721$ and the coefficients a 's are polynomial expression of the vibrational quantum number

$$a_i = \sum_{j=0} p_{ij} v^j \quad (11)$$

where the coefficients are in Table 1.

TABLE 1

	$i = 0$	$i = 1$	$i = 2$
$j = 0$	-29.8534	-175.5599	526.1455
$j = 1$	0.4177	5.1058	-15.7695
$j = 2$	-3.7076×10^{-2}	-3.7157×10^{-2}	0.1186
$j = 3$	2.4664×10^{-3}		
$j = 4$	-6.9381×10^{-5}		
$j = 5$	8.6006×10^{-7}		
$j = 6$	-3.9160×10^{-9}		

The model has been applied to investigate the behavior of different dissociation–recombination models on the flow properties of a dissociating–recombination mixture in the conic nozzle reported in Figure 5. We compare in particular the two kinetic models (QCT and LC) for a reservoir pressure $P_0 = 1$ atm and a reservoir temperature $T_0 = 8000$ K. In this condition the dissociation degree is around 90%, so that the recombination process is very strong and the differences between the two dissociation–recombination models should be important.

In general, the vibrational kinetics weakly affects the macroscopic quantities such as flow speed, temperature, and pressure profiles because the energy exchanged in the vibrational processes is small, this point being confirmed by the present calculations. As an example Figure 6 reports the trend of the

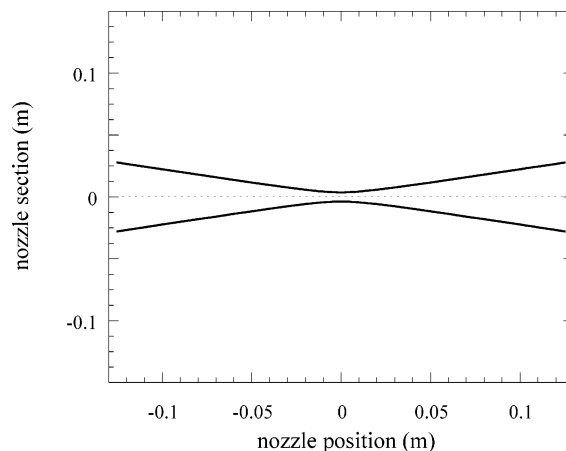


Figure 5. Nozzle section profile.

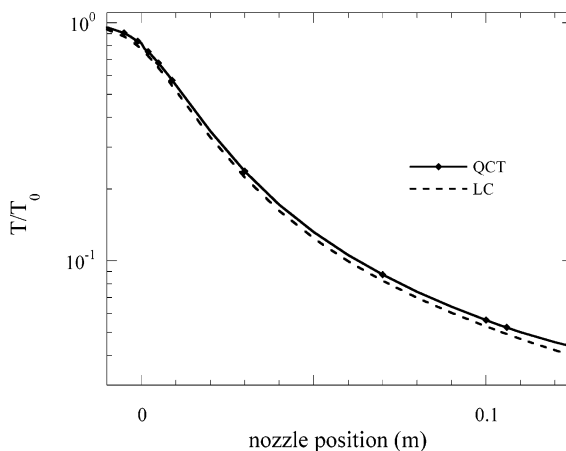


Figure 6. Temperature profile in the nozzle outlet for QCT and LC models. $T_0 = 8000$ K. $P_0 = 1$ atm.

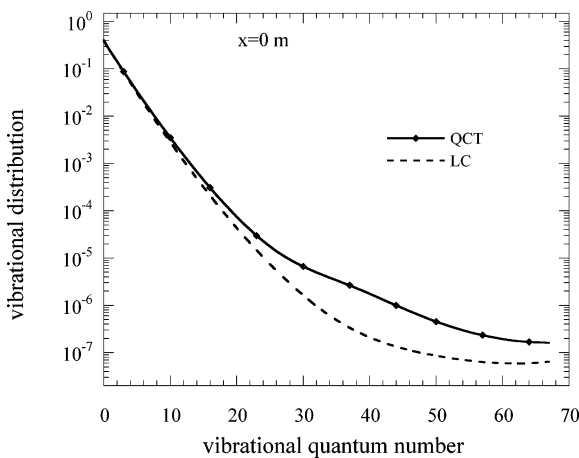


Figure 7. vdf 's at the nozzle throat ($x = 0$) for QCT and LC models. $T_0 = 8000$ K. $P_0 = 1$ atm.

translational temperature normalized to the initial one along the nozzle axis calculated according to the two dissociation models. We note a strong decrease of the translational temperature during the expansion, the results being not too sensitive to the adopted dissociation model.

More interesting is the behavior of the vibrational distributions and of the dissociation rates along the nozzle axis. This point can be appreciated in Figures 7–9 where we have reported the vibrational distributions of nitrogen for different nozzle positions. The reported behavior shows a large dependence of the results on the adopted model (LC, QCT). Qualitatively, the two

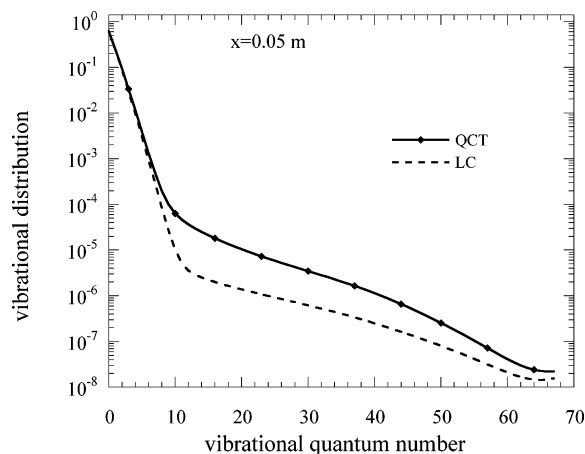


Figure 8. vdf's at the $x = 0.05$ m for QCT and LC models. $T_0 = 8000$ K. $P_0 = 1$ atm.

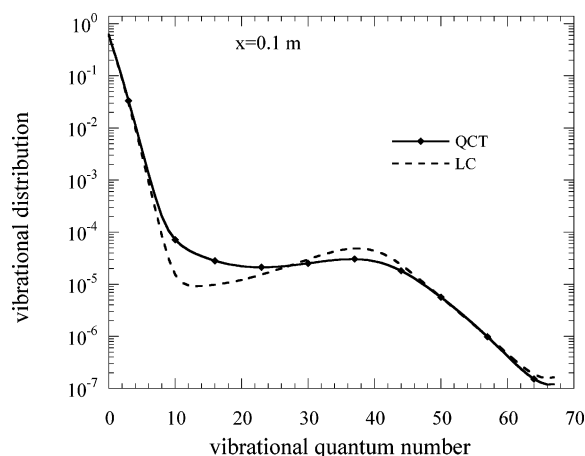


Figure 9. vdf's at the $x = 0.1$ m for QCT and LC models. $T_0 = 8000$ K. $P_0 = 1$ atm.

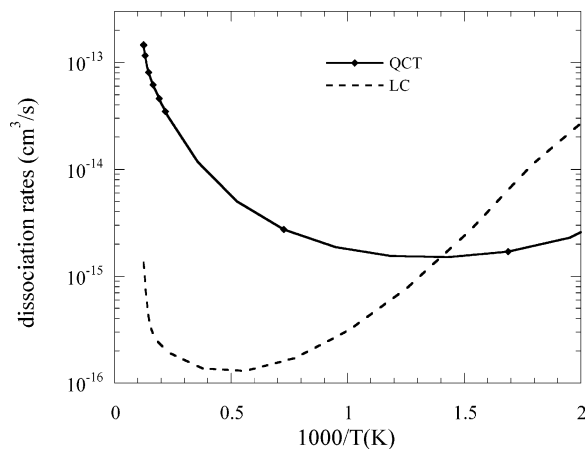


Figure 10. Arrhenius plot of the global dissociation rate for process 9 for QCT and LC models. $T_0 = 8000$ K. $P_0 = 1$ atm.

models show the same trend emphasizing large nonequilibrium vibrational distributions far from the nozzle throat. In particular, at the exit of the nozzle we can observe a long plateau in the vibrational distribution created by the recombination process, a result widely discussed in our previous calculations.^{7,15}

Let us now examine the dissociation rate induced by collisions of vibrationally excited molecules with atomic nitrogen along

the nozzle axis (see Figure 10). We plot these rates as a function of the inverse of the instantaneous translational temperature (Figure 6) which heavy particles undergo along the nozzle axis, i.e., we are representing the rates in an Arrhenius-type plot. The results, which are strongly dependent on the adopted model, show a large non-Arrhenius behavior of the dissociation rates as a consequence of non-Boltzmann vibrational distributions previously discussed. Note in fact that the dissociation rate can increase by decreasing the translational temperature, this behavior being dramatic with the LC model.

4. Conclusions

We have presented a detailed study of the state-to-state dissociation cross sections and rates for vibrationally rotationally excited nitrogen molecules induced by atomic nitrogen as well as corresponding $V-T_a$ rates. These data combined with the corresponding $V-V$ and $V-T$ rates calculated many years ago in refs 1 and 2 have been used in the 1D code describing the expansion of a $N_2(v)/N$ mixture along a converging-diverging nozzle. The results show interesting nonequilibrium vibrational distributions and non-Arrhenius behavior of dissociation rates along the nozzle axis.

As a conclusion, we want to point out that sophisticated kinetic models for aerospace applications can be now implemented in fluiddynamic codes thanks to the efforts made in the literature to calculate complete sets of state-to-state rates. Implementation of these models taking into account the ionization reaction will demand a parallel effort toward molecular physics describing electron and ion molecule reaction.^{14,16,17}

Acknowledgment. The present paper has been partially supported by MIUR under contracts (PRIN) "Dinamica Molecolare di processi elementari in condizioni di non equilibrio", (FIRB) "Dinamica microscopica della reattività chimica" and (FISR) "Modellistica molecolare di sistemi di complessità crescente". The authors thank Dr. A. Casavola for help in data fitting.

References and Notes

- Capitelli, M.; Gorse, C.; Billing, G. D. *Chem. Phys.* **1980**, *52*, 299.
- Billing, G. D. Topics in Current Physics, In *Nonequilibrium Vibrational Kinetics*; Capitelli, M., Ed.; Springer-Verlag: New York, 1986; Vol. 86, Chapter 4.
- Laganà, A.; Garcia, E. *J. Phys. Chem.* **1994**, *98*, 502.
- Esposito, F.; Capitelli, M.; Gorse, C. *Chem. Phys.* **2000**, *257*, 193.
- Esposito, F.; Capitelli, M. *Chem. Phys. Lett.* **2002**, *364*, 180.
- Cacciatore, M.; Rutigliano, M.; Billing, G. D. *J. Thermophys. Heat Transfer* **1999**, *13*, 195.
- Colonna, G.; Capitelli, M. *J. Phys. D: Appl. Phys.* **2001**, *34*, 1812.
- Esposito, F.; Gorse, C.; Capitelli, M. *Chem. Phys. Lett.* **1999**, *303*, 636-640.
- Laganà, A.; Garcia, E.; Ciccarelli, L. *J. Phys. Chem.* **1987**, *91*, 312.
- Esposito, F. Ph.D. Thesis, Università degli Studi, Bari **1999** (Italy).
- Roberts, R. E.; Bernstein, R. B.; Curtiss, C. F. *J. Chem. Phys.* **1969**, *50*, 5163.
- Schwenke, D. W. *J. Chem. Phys.* **1990**, *92*, 7267.
- Nikitin, E. E. Theory of Elementary Atomic and Molecular Processes in Gases, Clarendon Press: Oxford, 1974; Chapter 7.
- AVOGADRO database on rate constants of chemical and plasma-chemical reactions, RRATE AVOGADRO Centre, Institute of Mechanics, Moscow State University, Moscow, Russia, 1992-1995.
- Colonna, G.; Tuttafesta, M.; Giordano, D. *Comput. Phys. Comm.* **2001**, *138*, 213.
- Capitelli, M.; Ferreira, C. M.; Gordiets, B. F.; Osipov, A. I. *Plasma Kinetics in Atmospheric Gases*; Springer Series on Atomic, Optical and Plasma Physics; Springer-Verlag: Berlin, Heidelberg, 2000.
- Frost, M. J.; Kato, S.; Bierbaum, V. M.; Leone, S. R. *J. Chem. Phys.* **1994**, *100*, 6359.